

Fluorescent Self-Assembled Polyphenylene Dendrimer Nanofibers

Daojun Liu,[†] Steven De Feyter,^{*,†} Mircea Cotlet,[†] Uwe-Martin Wiesler,[‡]
Tanja Weil,[‡] Andreas Herrmann,[‡] Klaus Müllen,[‡] and Frans C. De Schryver^{*,†}

Laboratory for Photochemistry and Spectroscopy, Department of Chemistry, Katholieke Universiteit Leuven (KU Leuven), Celestijnenlaan 200F, B-3001 Leuven, Belgium, and Max Planck Institute for Polymer Research, Ackermannweg 10, 55128 Mainz, Germany

Received June 24, 2003

ABSTRACT: A second-generation polyphenylene dendrimer **1** self-assembles into nanofibers on various substrates such as HOPG, silicon, glass, and mica from different solvents. The investigation with noncontact atomic force microscopy (NCAFM) and scanning electron microscopy (SEM) shows that the morphology of the dendrimer nanofibers highly depends on substrate, solvent, and preparation method. Fluorescent nanofibers can be prepared from a polyphenylene dendrimer with chromophores either attached to the periphery of the dendrimer or incorporated in its core. Fluorescent nanofibers formed from polyphenylene dendrimer **4** with a perylenediimide core show isolated-chromophore emission due to the shielding of the rigid polyphenylene dendrons. Dendrimer **2** with one perylenemonoimide attached to its periphery self-assembles into fluorescent nanofibers, which exhibit a dimer like emission as a result of the interactions between peripheral chromophores. Dendrimer **3** with two perylenemonoimides at the rim does not form nanofibers by itself, but mixing of nonfluorescent dendrimer **1** with fluorescent dendrimers **2** or **3** leads to the formation of nanofibers with a homogeneous composition. Therefore, mixing can not only coassemble nonnanofiber-forming dendrimer **3** into nanofibers but also give rise to isolated-chromophore emission upon proper dilution.

Introduction

Dendrimers have attracted much attention for the past two decades because of their fascinating structure and unique properties such as their globular shape, highly controlled size, radially controlled chemical composition, multivalent periphery, and variable inner volume.^{1–4} Self-assembly of dendrimers with or without guest molecules at the ensemble^{5–10} as well as the single molecule level¹¹ is of special interest because this creates a wide collection of novel structures and surfaces with higher complexity and promising properties.

The self-assembly of dendrimers into mono- or multilayers on a solid substrate through electrostatic interactions,^{12–16} polydentate interactions,^{17–21} or covalent bonding²² has been investigated. The self-assembled dendrimer mono- or multilayers were found to exhibit unique properties and potential applications such as their use as nanoreservoirs,¹⁵ as molecular gate membranes,^{17a} and as effective resists for high-resolution lithography.^{22b} With the techniques of microcontact printing (μ CP) and dip-pen nanolithography, dendrimer molecules have been patterned on a substrate surface,^{23–25} which also allows the subsequent postfunctionalization for the fabrication of patterned nanostructures.

Dendrimers can also self-assemble into three-dimensional nanostructures. Tomalia and co-workers²⁶ have reported the self-assembly of PAMAM dendrimers into supramolecular core-shell dendrimer assemblies with higher complexity and dimensions. Percec and co-workers²⁷ have reported the self-assembly of monodendritic building blocks in bulk into spherical, cylindrical,

and more complex supramolecular and supramacromolecular dendrimers. Masuhara²⁸ and Schlüter²⁹ also investigated self-assembled nanostructures from dendronized polymers, a type of dendrimer with multiple functional polymer cores.

Lamellar patterns formed via the side-by-side arrangement of linear polyphenylenes³⁰ and columns built from face-to-face polycyclic aromatic hydrocarbons (PAHs) due to the π - π interactions³¹ have been described as typical supramolecular patterns of benzene-based macromolecules. Polyphenylene dendrimers are a special class of dendrimers,^{3,32} which are characterized by their shape-persistent 3D structures.^{33,34} Polyphenylene dendrimers have been observed to form several hundred nanometer long organized structures when additional alkyl chains are attached to their periphery³⁵ as well as dendrimer multilayers with gold nanoparticles.²⁰

We have recently reported that polyphenylene dendrimers with various cores (such as tetraphenylmethane, biphenyl, and azobenzene) and of different generations can self-assemble into micrometer long nanofibers in addition to the formation of globular dendrimer aggregates, on hydrophobic surfaces such as HOPG and silanized mica.³⁶ A special case is dendrimer **1** (Figure 1), a second-generation polyphenylene dendrimer containing a tetraphenylmethane core, which exclusively self-assembles into micrometer long nanofibers by drop-casting under controlled atmospheric conditions. A critical issue is the extent to which the polyphenylene dendrimers can be functionalized while still retaining their fiber-forming properties. What is the effect of modifying the dendrimer core? Will the dendrimers decorated at the rim with one or multiple functionalities still can form nanofibers? In this contribution, we investigate the effect of solvent, substrate, and controlled atmospheric conditions on the formation and morphology of the nanofibers. To get insight into the effect of functionalization, we have investigated the

* Corresponding authors: e-mail steven.defeyter@chem.kuleuven.ac.be or frans.deschryver@chem.kuleuven.ac.be; Fax (+32)-16-327989.

[†] Laboratory for Photochemistry and Spectroscopy.

[‡] Max Planck Institute for Polymer Research.

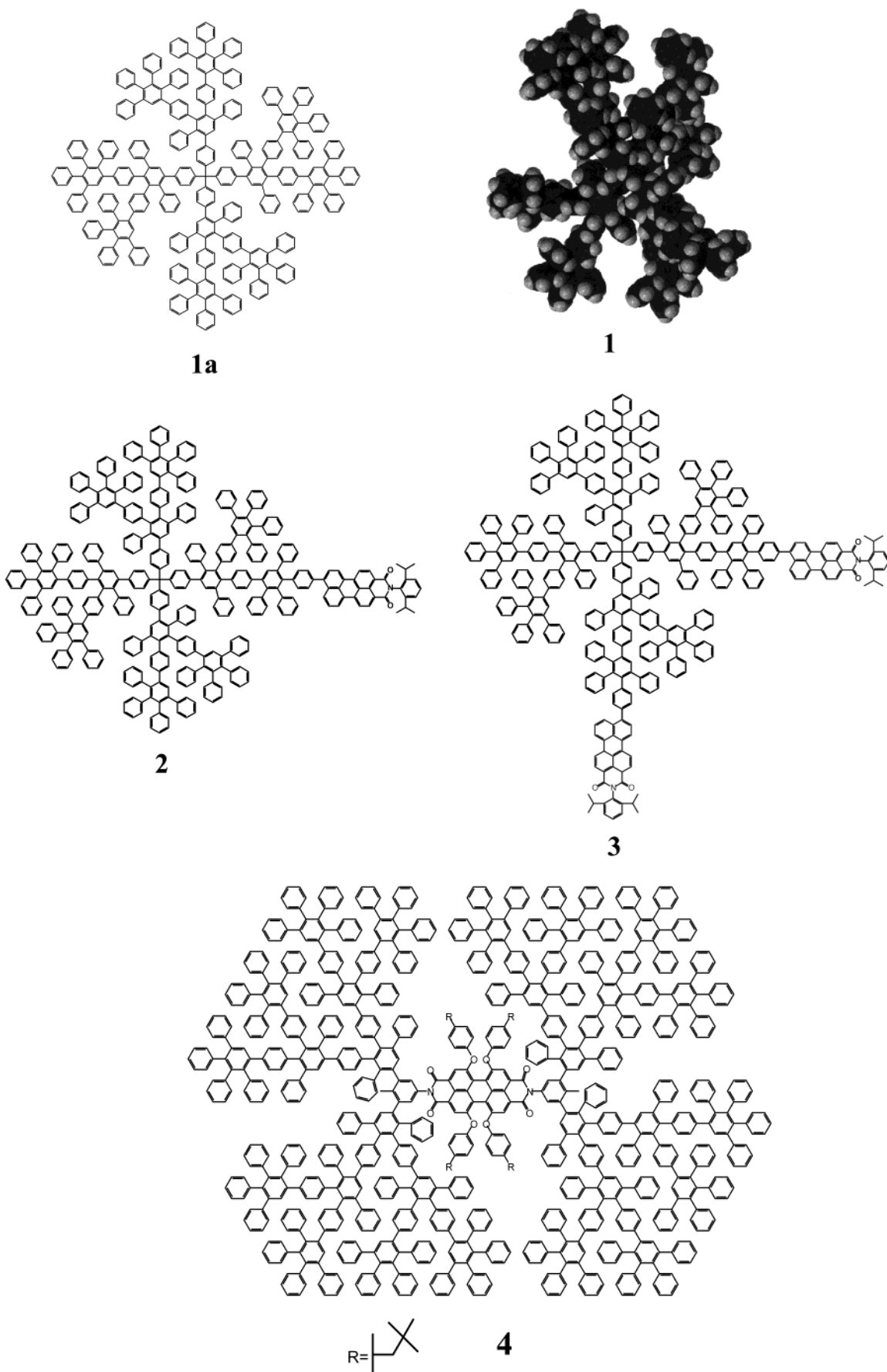


Figure 1. (1a) Molecular structure of polyphenylene dendrimer **1**. (1b) Space-filling view of dendrimer **1** built by a Merck Molecular Force Field (MMFF) method. (2, 3) Molecular structures of polyphenylene dendrimers with perylenemonoimide attached to the periphery. (4) Molecular structure of polyphenylene dendrimer with a perylenediimide core.

self-assembly properties of dendrimers functionalized with one or multiple fluorescent peryleneimide chromophores. We have explored the influence of the number and location of the chromophore(s) within the dendrimer and the effect of mixing with nonfunctionalized dendrimers.

Experimental Section

Chemicals. The synthesis of polyphenylene dendrimers 1–4 has already been reported.^{32,37,38} These dendrimers exhibit good solubility in common organic solvents and thus can be characterized by MALDI-TOF-MS. The perfect agreement between calculated and experimentally determined m/z ratios confirms its monodispersity. CHCl_3 (Acros Organics, Fair Lawn, NJ), THF (Acros Organics, Fair Lawn, NJ), acetone (Aldrich Chemical Co. Inc., Milwaukee, WI), and ethanol (BDH Laboratory Suppliers, Poole, England) were used as received. All the used solvents are of spectrophotometric grade.

Substrates. The HOPG and mica were freshly cleaved immediately before use. The glass and silicon substrates, which have an oxide layer of several nanometers, were pretreated for 10 min in an ultrasonic bath at 25 °C in acetone and then cleaned in a piranha solution (7:3 mixture of concentrated sulfuric acid and 30% hydrogen peroxide) at 70 °C for 30 min. After the treatment, the substrate was thoroughly rinsed with Milli-Q water and blow-dried with nitrogen.

Sample Preparation. Assemblies of dendrimers were prepared on the surface of substrates by drop casting. Briefly, a substrate was put in a nearly closed glass container (20 cm \times 8 cm \times 20 cm) with preadded organic solvent (or mixture of water and organic solvent) in order to create a saturated solvent environment. Then five drops (ca. 150 μL) of dendrimer solution (see figure captions for concentrations of dendrimer solutions) were deposited on the surface of substrate. The solvent evaporated slowly, typically within several hours, depending on the specific solvent.

Atomic Force Microscopy (AFM). Assemblies of polyphenylene dendrimers were visualized with AFM. AFM was performed with a Discoverer TMX2010 AFM system (ThermoMicroscopes, San Francisco, CA) operating in noncontact mode using Si probes (ThermoMicroscopes, San Francisco, CA) with a spring constant of 34–47 N/m and a resonance frequency of 174–191 kHz. A calibration silicon grating (TGZ01, pitch 3 μm , $\Delta z = 26 \pm 1$ nm, MicroMasch, Tallinn, Estonia) was used to calibrate the piezo scanner. Measurements were done under ambient conditions. Image analysis was performed with Topometrix SPMLab 5.0.

Scanning Electron microscope (SEM). Assemblies of dendrimer 1 on the silicon substrate were also visualized with a SEM (JEOL TSM-5600). SEM was performed with an acceleration voltage of 15 kV and, in a few cases, at a tilted angle.

Confocal Fluorescence Microscopy. Picosecond time-resolved confocal fluorescence detection and spectroscopy from dendrimer nanostructures was performed using an optical setup that is described elsewhere.³⁹ Briefly, samples on a silicon substrate were mounted on an Olympus IX 70 inverted microscope equipped with a scanning stage (Physics Instruments, Waldbronn, Germany). Excitation with the 488 nm pulsed laser line, achieved by frequency-doubling the output of a mode-locked picosecond Ti:sapphire laser (Tsunami Spectra Physics) pumped by an Ar⁺ laser (BeamLok 2080 Spectra Physics), occurred through a dry objective lens (0.85 NA, $\times 63$, Zeiss). Fluorescence was collected by the same objective, passed through a dichroic mirror (DRLP495 Chroma Technology, Brattleboro, NY), filtered through a notch filter (Kaiser Optical Systems, Ann Arbor, MI), and simultaneously focused, via a 50 μm pinhole and a 50–50% nonpolarizing beam splitter cube, on an avalanche photodiode (APD) (SPCM 15, EG & G, Quebec) and into the entrance of a polychromator (Acton SP 150) coupled to a cooled charge-coupled device camera (Princeton Instruments). The signal from the APD was input into a time-correlated single photon counting PC card (SPC 630,

Picoquant GmbH). The fluorescence decays were analyzed with a homemade program that uses a reweighted iterative reconvolution method based on the Marquadt algorithm. The goodness of the fits were judged by the values of the reduced χ^2 as well as by inspecting the residual function graphs for each fitted data set.

Molecular Modeling. Geometry optimization of the dendrimer 1 was performed in a vacuum by a molecular mechanics method (Merck Molecular Force Field)⁴⁰ in Spartan (Wave Function Inc., Irvine, CA).

Results and Discussion

Self-Assembled Polyphenylene Dendrimer 1 Nanofibers on Various Substrates. We have shown in previous papers³⁶ that polyphenylene dendrimers with a well-defined 3D structure can self-assemble into fibrillar nanostructures. Most of these polyphenylene dendrimers self-assemble into micrometer long nanofibers, along with the formation of globular dendrimer aggregates, on a hydrophobic surface such as a HOPG or silanized mica. In this section, we explore the effect of deposition conditions and substrate properties on the formation of self-assembled structures by dendrimer 1, of which we have demonstrated the formation of nanofibers under controlled conditions previously.^{36b}

Figure 2A shows a representative AFM image of nanofibers formed from dendrimer 1 by drop-casting from a CHCl_3 solution on a HOPG surface. Dendrimer 1 *exclusively* self-assembles into fibrillar nanostructures under controlled atmospheric conditions (see Experimental Section). In addition to the formation of discrete nanofibers, most of the nanofibers aggregate into bundles forming clusters (Figure 2B). The length of the nanofibers is typically less than 10 μm . On a silicon surface, bigger nanofiber clusters composed of nanofibers with a length of tens of micrometers were obtained. The diameter of these clusters ranges from 10 to 200 μm as revealed by AFM and SEM measurements. Typical AFM and SEM images of a dendrimer 1 nanofiber cluster on a silicon surface are shown in parts C and D of Figure 2, respectively.

The ordering of nanofibers into clusters is considered to be the result of dewetting. Because of the dewetting in the course of the evaporation process, the dendrimer solution evolves into separated domains,⁴¹ within which the nanofibers form and aggregate into clusters. The area around the nanofiber cluster in Figure 2C is almost free of dendrimer molecules. Because of the difficulty of preparing a mesoscale flat HOPG surface by cleaving and the presence of numerous steps and kinks over large dimensions, the HOPG surface should be rougher than that of the silicon. This could lead to the formation of smaller and more domains of droplets of dendrimer in solution at the HOPG surface toward the end of the solvent evaporation, which could explain the fact that smaller and more dendrimer nanofiber clusters as well as discrete nanofibers are formed on the surface of HOPG compared to a silicon surface (Figure 2A,C).

When THF was used as the solvent, the nanofibers prepared by drop-casting on a silicon surface were observed to be quite evenly distributed, and they formed a network extending over the entire substrate surface. A representative AFM image of a dendrimer 1 nanofiber network formed under such experimental conditions is shown in Figure 3A. There is substantial aggregation of the dendrimer nanofibers into nanofiber bundles (Figure 3B). The rather homogeneous distribution of the nanofibers formed from THF solution on the silicon

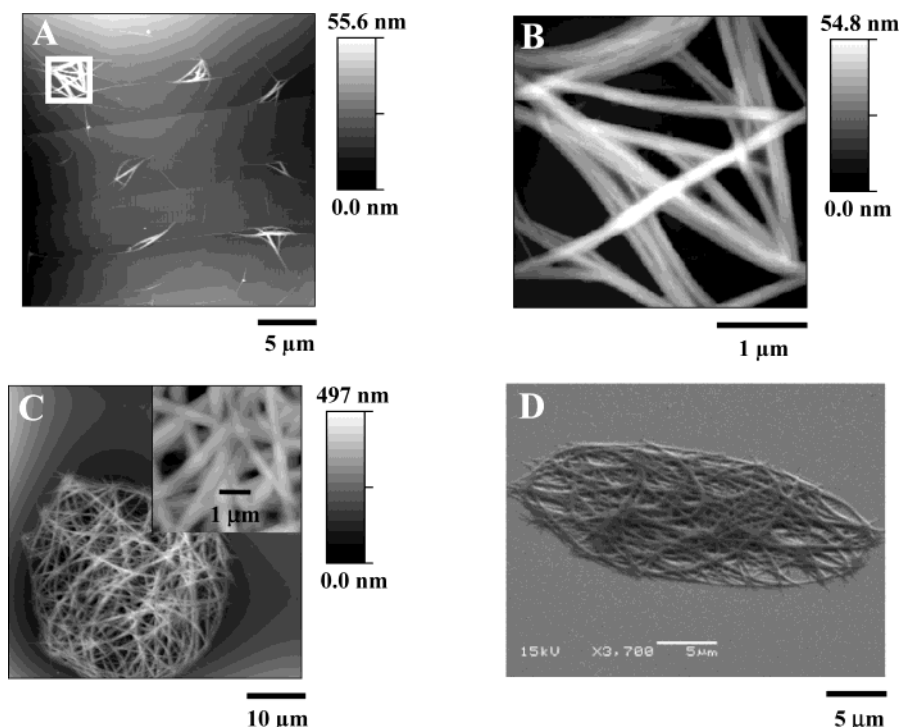


Figure 2. (A) NCAFM image ($25\ \mu\text{m} \times 25\ \mu\text{m}$) of dendrimer **1** nanofibers prepared by drop-casting a 1.0×10^{-5} M dendrimer **1** solution in CHCl_3 on a HOPG surface. (B) A smaller scale NCAFM image ($3.5\ \mu\text{m} \times 3.5\ \mu\text{m}$) of a dendrimer **1** nanofiber cluster in part A indicated by a frame. (C) NCAFM image ($50\ \mu\text{m} \times 50\ \mu\text{m}$) of a dendrimer **1** nanofiber cluster prepared by drop-casting a 1.0×10^{-5} M dendrimer **1** solution in CHCl_3 on a silicon surface. A smaller scale AFM image ($5\ \mu\text{m} \times 5\ \mu\text{m}$) is shown in the inset. (D) SEM image of a dendrimer **1** nanofiber cluster on a silicon surface imaged at a tilted angle of 70° .

surface could be ascribed to the improved wetting properties of THF toward the oxidized silicon surface, which results in a thin dendrimer solution layer rather than separated domains at the final stage of the solvent evaporation.

It was found that the addition of a small amount of water to the THF atmosphere during the drop-casting suppressed the aggregation of nanofibers. Parts C and D of Figure 3 show AFM images of the nanofibers formed from a dendrimer **1** solution in THF in a saturated atmosphere of THF and 5% and 10% (v/v) H_2O , respectively. In the presence of 10% water, a large number of individual curved nanofibers is obtained with many crossing points (Figure 3E,F). The topography profile in Figure 3E shows that the nanofibers formed have a height of tens of nanometers. Since water can completely wet the oxidized silicon surface, the presence of water will certainly improve the wetting properties of the mixed solvent with THF and thus decrease the shear force of the lateral flow of the solvent. This might explain why less aggregated dendrimer nanofiber bundles are observed with increasing amount of water (Figure 3A,C,D). Upon increasing the water content in the mixed solvent atmosphere to 20%, straighter nanofibers were obtained, which evolve into "star"-shaped networks, as indicated by the AFM and SEM images in Figure 3G–I. The SEM image in Figure 3I shows that the nanofibers are still well-separated even in the center of the "star", suggesting that the nanofiber networks did not grow divergently from the center but were formed as a result of the convergent aligning of the preformed nanofibers.

The morphology of the nanofibers formed by drop-casting a dendrimer **1** solution in THF on a silicon surface was also dependent on the water content in the mixed vapor atmosphere. With less than 10% water, the

nanofibers have a round cross section (Figure 3B). With increasing water content, the surfaces of nanofibers become more flat, as indicated by the topography profile in Figure 3E (10% water). When the water content was increased to 20%, nanoribbons with a flat surface were clearly observed as reported in Figure 3H and the related topography profile. Some nanoribbons are tilted relative to the substrate surface. Comparison between the dimensions of these nanofibers obtained by AFM and SEM supports the formation of nanoribbons. As can be seen from the topography profiles in Figure 3H, the height of the nanoribbons is typically less than 100 nm, whereas the width of the nanoribbons presented in Figure 3I is around 200 nm. Increasing further the water content to about 40% results in an irreproducible nanofiber structure. Above 40% water content, only globular aggregates of dendrimer **1** were observed as a result of the rapid evaporation of THF. The globular aggregates formed from dendrimer **1** solution in THF in a pure water vapor environment are shown in Figure 3J.

It should be pointed out that since the glass and mica substrates have similar surface properties as silicon, the formation of nanofiber networks of dendrimer **1** on these two substrates was also observed, and representative AFM images are shown in parts A and B of Figure 4, respectively.

Formation of Fluorescent Nanofibers from Functionalized Polyphenylene Dendrimers. (A) **Self-Assembly of Monochromophoric and Multichromophoric Dendrimers.** Dendrimer **2** only differs from dendrimer **1** in the presence of a perylenemonoimide chromophore covalently linked to the polyphenylene arms of the dendrimer periphery. It was hoped that the attachment of this chromophore would not influence the self-assembling behavior too much as dendrimer **1** has

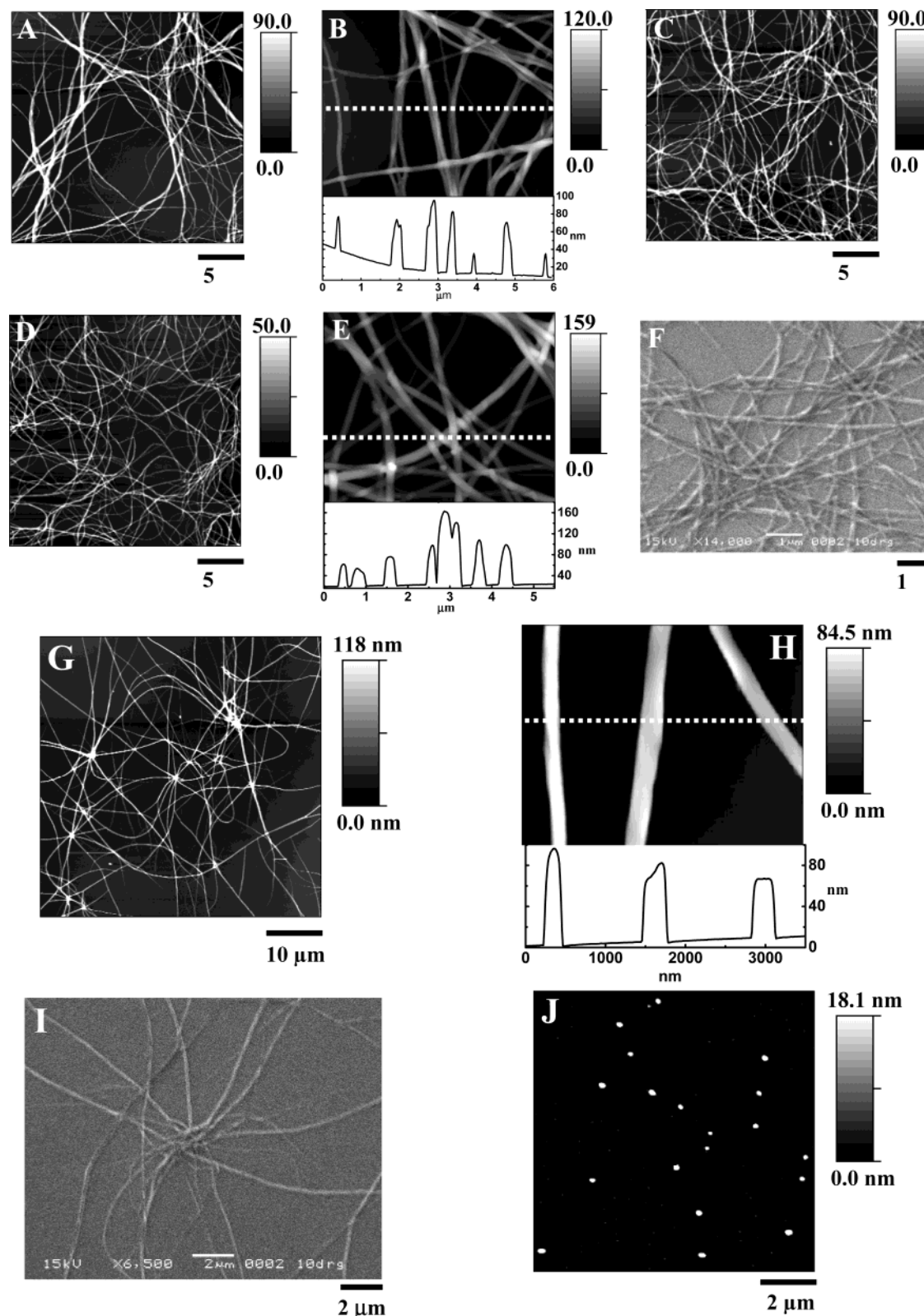


Figure 3. (A) NCAFM image ($25\ \mu\text{m} \times 25\ \mu\text{m}$) of dendrimer **1** nanofibers prepared by drop-casting a $2.0 \times 10^{-6}\ \text{M}$ dendrimer **1** solution in THF on a silicon surface in a saturated environment of THF. (B) A smaller scale NCAFM image of part A. Topography profile along the dotted line indicated in the image is shown beneath. (C) NCAFM image ($25\ \mu\text{m} \times 25\ \mu\text{m}$) of dendrimer **1** nanofibers prepared by drop-casting a $2.0 \times 10^{-6}\ \text{M}$ dendrimer **1** solution in THF in a saturated environment of THF:H₂O = 95:5 (v/v) on a silicon surface. (D) NCAFM image ($25\ \mu\text{m} \times 25\ \mu\text{m}$) of dendrimer **1** nanofibers prepared by drop-casting a $2.0 \times 10^{-6}\ \text{M}$ dendrimer **1** solution in THF in a saturated environment of THF:H₂O = 90:10 (v/v) on a silicon surface. (E) A smaller scale NCAFM image of part D. Topography profile along the dotted line indicated in the image is shown beneath. (F) SEM image of part D. (G) NCAFM image ($50\ \mu\text{m} \times 50\ \mu\text{m}$) of dendrimer **1** nanofibers prepared by drop-casting a $2.0 \times 10^{-6}\ \text{M}$ dendrimer **1** solution in THF in a saturated environment of THF:H₂O = 80:20 (v/v) on a silicon surface. (H) A smaller scale NCAFM image of part G. Topography profile along the dotted line indicated in the image is shown beneath. (I) SEM image of part G. (J) NCAFM image ($10\ \mu\text{m} \times 10\ \mu\text{m}$) of dendrimer **1** aggregates prepared by drop-casting a $2.0 \times 10^{-6}\ \text{M}$ dendrimer **1** solution in THF at a saturated H₂O environment on a silicon surface.

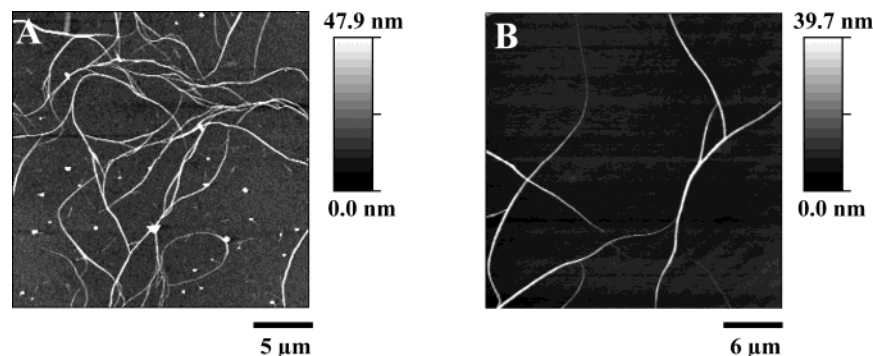


Figure 4. NCAFM image of dendrimer **1** nanofibers prepared by drop-casting a 2.0×10^{-6} M dendrimer **1** solution in THF in a saturated environment of THF:H₂O = 90:10 (v/v) on a glass surface (A, $25 \mu\text{m} \times 25 \mu\text{m}$) and on a mica surface (B, $30 \mu\text{m} \times 30 \mu\text{m}$).

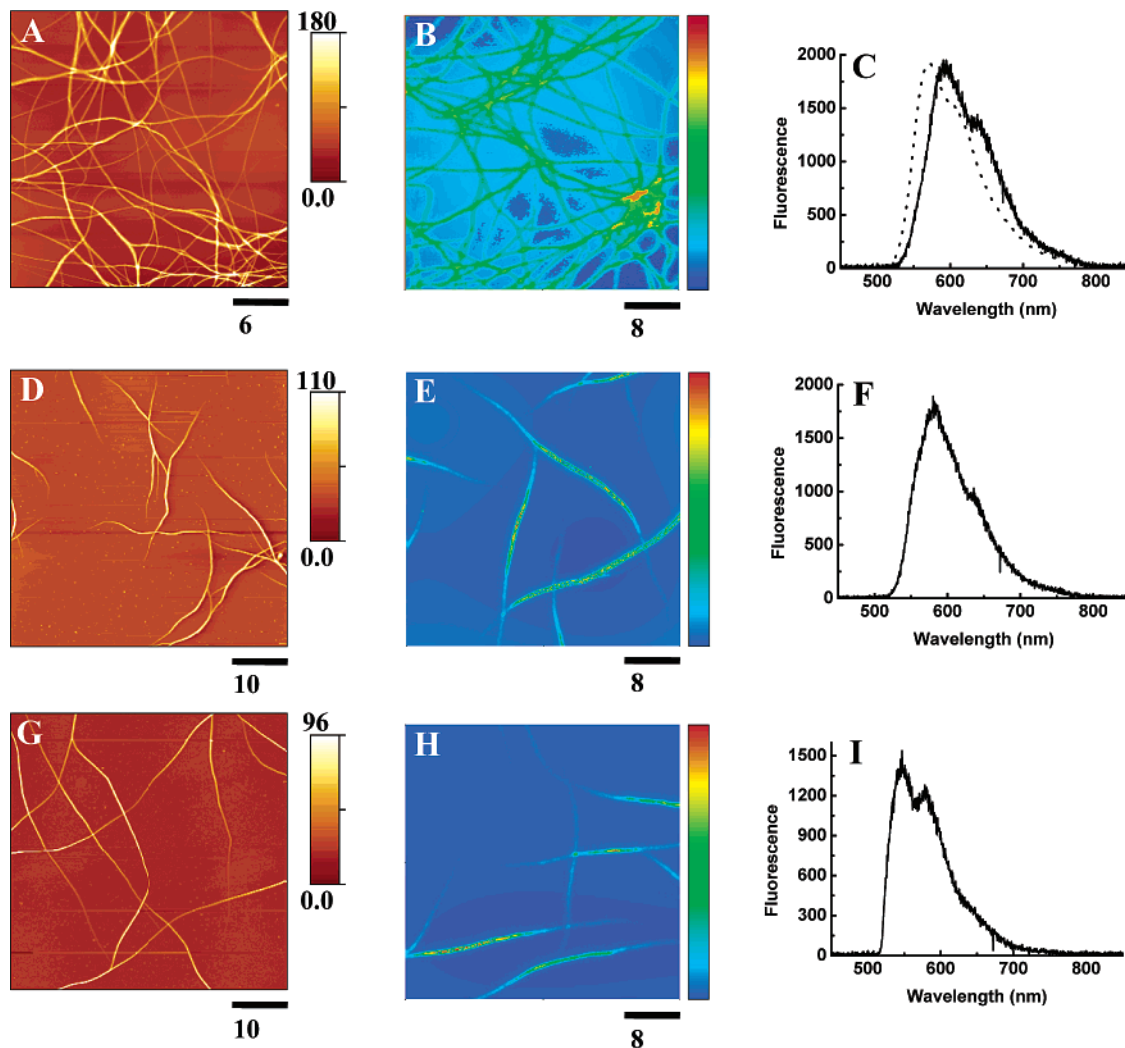


Figure 5. NCAFM image (A, $30 \mu\text{m} \times 30 \mu\text{m}$), confocal fluorescence image (B, $40 \mu\text{m} \times 40 \mu\text{m}$), and the emission spectrum (C) of dendrimer **2** nanofibers; NCAFM image (D, $50 \mu\text{m} \times 50 \mu\text{m}$), confocal fluorescence image (E, $40 \mu\text{m} \times 40 \mu\text{m}$), and the emission spectrum (F) of dendrimers **1** and **2** mixed (molar ratio, 5:5) nanofibers; NCAFM image (G, $50 \mu\text{m} \times 50 \mu\text{m}$), confocal fluorescence image (H, $40 \mu\text{m} \times 40 \mu\text{m}$), and the emission spectrum (I) of dendrimers **1** and **2** mixed (molar ratio, 9:1) nanofibers. All nanofibers are prepared by drop-casting a 2.0×10^{-6} M (total concentration) dendrimer solution in THF on a silicon surface in a saturated environment of THF:H₂O = 90:10 (v/v). The emission spectrum (excitation wavelength 488 nm) of dendrimer **1** in THF is shown as a dotted line in (C).

excellent self-assembling properties, and there are no specific interactions between this rather small chromophore and the rigid dendrimer. Figure 5A is an AFM image of the self-assembled structures formed by dendrimer **2** on a silicon surface under a saturated mixed solvent environment (THF:H₂O = 9:1). Indeed, functionalized dendrimer **2** by itself exclusively self-assembles into nanofibers as well, with dimensions similar

to those of nanofibers formed from dendrimer **1** under similar experimental conditions. In contrast, no well-defined nanofibers have been visualized from functionalized dendrimer **3** with more chromophores (peryleneimides) attached to its periphery (vide infra). The dendrimer nanofibers formed from dendrimer **2** are fluorescent, as shown by fluorescence confocal microscopy image in Figure 5B. The sample was excited at 488

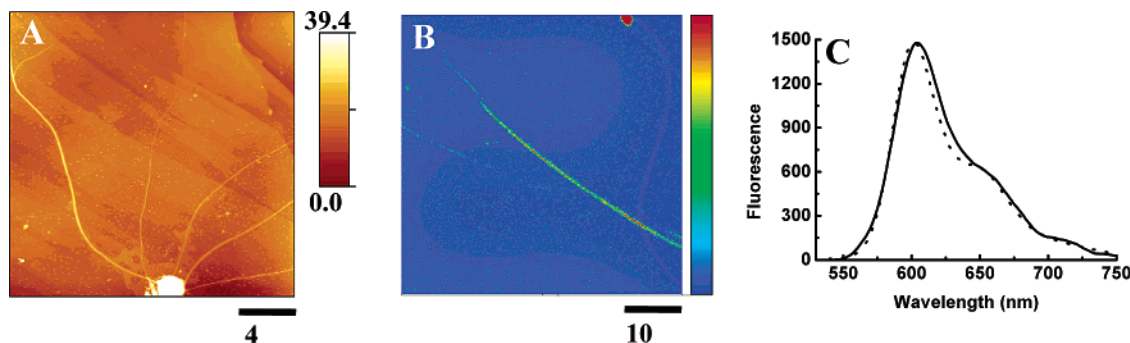


Figure 6. NCAFM image (A, $20\ \mu\text{m} \times 20\ \mu\text{m}$), confocal fluorescent image ($50\ \mu\text{m} \times 50\ \mu\text{m}$), and the emission spectrum (C) of nanofibers prepared by drop-casting a 1.0×10^{-5} M dendrimer **4** solution in CHCl_3 on a HOPG surface in a saturated CHCl_3 atmosphere. The emission spectrum of dendrimer solution in CHCl_3 is shown as a dotted line in (C).

nm using linearly polarized light, and the fluorescence images were recorded along both a parallel and a perpendicular direction. No polarization effect was observed, which indicates that the dendrimers are not anisotropically aligned over distances that are equal to or exceed the diffraction limited spot under confocal conditions (~ 300 nm). Emission spectra of these nanofibers were also recorded and are shown in Figure 5C. In comparison with the fluorescence spectra of isolated dendrimers in solution, these nanofibers showed emission with a maximum around 600 nm (compared to the fluorescence maximum around 570 nm in solution), suggesting strong interactions between chromophores within these nanofibers. The fluorescence of these nanofibers is characterized by multiexponential decays with a contribution of a decay component longer than 5 ns, indicative of perylenemonoimide dimer-like emission.⁴² As the perylenemonoimide chromophores are linked to the periphery of dendrimers, there is quite a large possibility that they can interact.

Dendrimer **4** (structure shown in Figure 1), where a fluorescent perylenediimide function is buried deep inside the polyphenylene dendritic arms, was then employed. Decoration of perylenediimide with polyphenylene dendrons can not only increase its solubility in common organic solvents but also make its aggregation less likely.³⁸ The formation of micrometer long nanofibers from dendrimer **4** was also expected since we have demonstrated that the interactions among polyphenylene dendritic arms lead to the formation of micrometer long polyphenylene dendrimer nanofibers.^{36b} Indeed, a typical AFM image of nanofibers, together with globular aggregates, formed from dendrimer **4** is shown in Figure 6A. As expected, the self-assembled nanofibers from dendrimer **4** are fluorescent, as evidenced by the fluorescence image (Figure 6B) visualized using confocal microscopy. In contrast to the nanofibers formed by dendrimer **2**, the fluorescence spectra of those of dendrimer **4** are (almost) identical to spectra obtained in diluted solutions of **4** (Figure 6C). No red-shifted emission of these solid-state nanofibers was observed compared to the emission spectra of dendrimer **4** in solution.⁴³ This indeed proves that the chromophores are shielded from each other in the dendrimer nanofibers as well.³⁸ It should be pointed out that the formation of these fluorescent nanofibers is always accompanied by the formation of globular aggregates, and its formation is mainly limited to hydrophobic substrates such as HOPG and silanized mica.

(B) Self-Assembly of Mixtures of Dendrimers.

Dendrimer **2** exclusively self-assembles into micrometer long nanofibers, and by fluorescence spectroscopy, it was

shown that interaction of the dendrimers within the nanofibers is observed by the dimer-like emission of the dyes. The question arises what will happen if mixtures of fluorescent and nonfluorescent dendrimers are let to self-assemble. Will this lead to the formation of "mixed" nanofibers or other mixed self-assembled structures, or will the dendrimers phase separate? Since both non-fluorescent dendrimer **1** and fluorescent dendrimer **2**, which have the same dendrimer structure, self-assemble into nanofibers under the same experimental conditions, mixtures of these dendrimers in different concentration ratios were investigated. It was observed that mixtures of dendrimers **1** and **2** exclusively lead to the formation of nanofibers (vide supra). The AFM, fluorescence images, and the emission spectra of such nanofibers formed from two mixtures with different concentration ratios are shown in Figure 5D–I. The main difference between the results based on different concentration ratios are the respective emission spectra. Upon increasing the concentration ratio of the nonfluorescent dendrimer **1** over the fluorescent dendrimer **2**, the fluorescence spectrum shifts to the blue (Figure 5C,F,I), and the spectrum in Figure 5I shows a clear vibrational fine structure which is typical for the emission of isolated perylenemonoimide chromophores. Since (1) the exclusive formation of nanofibers from the dendrimer mixtures as shown from the AFM images, (2) the predominant and rather homogeneous emission from these nanofibers, and (3) the change in the fluorescence spectrum toward monomer-like emission upon decreasing the ratio of fluorescent over nonfluorescent chromophores, we can conclude that there is homogeneous mixing of dendrimers **1** and **2** within the nanofibers over the length scale of optical resolution in confocal microscopy. Mixing dendrimers can also be used to form nanofibers even if one of the dendrimers does not form nanofibers by itself. Dendrimer **3** (structure shown in Figure 1) has the same backbone structure as dendrimer **1** but with two perylenemonoimide chromophores attached to the periphery. When dendrimer **3** solution was drop-casted on a silicon surface, nanorods instead of well-defined nanofibers were formed (Figure 7A), which indicates that the presence of two perylenemonoimide moieties interferes with the self-assembling behavior and suppresses the formation of well-defined nanofibers. However, when a mixed solution of dendrimers **1** and **3** up to a ratio of 50% of **3** was drop-casted, these dendrimers exclusively self-assemble into well-defined nanofibers. The representative AFM and fluorescent images as well as the emission spectra of nanofibers formed from the dendrimers **1** and **3** under different mixing ratios are shown in Figure 7D–I. Similar to the

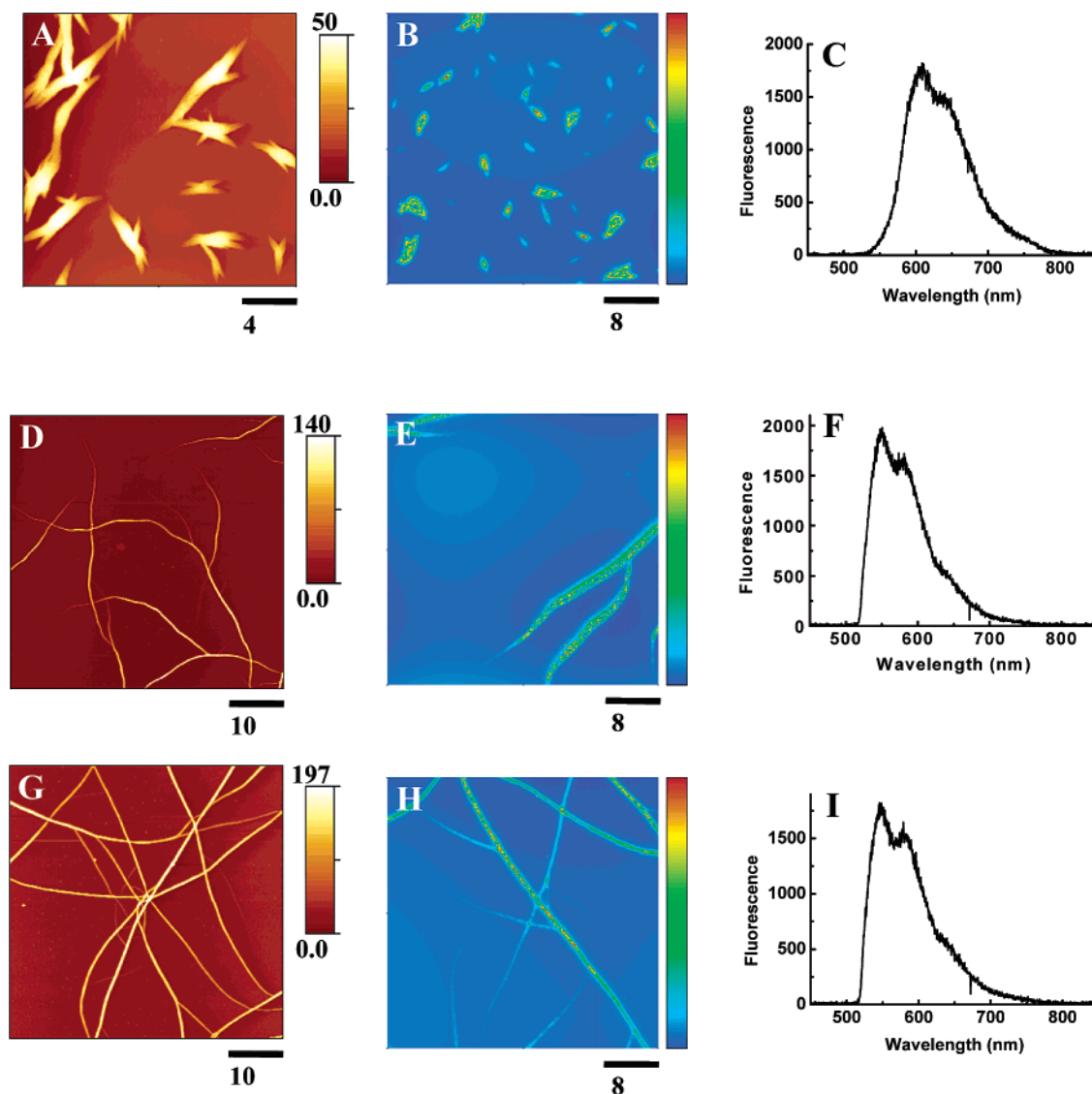


Figure 7. NCAFM image (A, $20\ \mu\text{m} \times 20\ \mu\text{m}$), confocal fluorescence image (B, $40\ \mu\text{m} \times 40\ \mu\text{m}$), and the emission spectrum (C) of dendrimer **3** nanoaggregates; NCAFM image (D, $50\ \mu\text{m} \times 50\ \mu\text{m}$), confocal fluorescence image (E, $40\ \mu\text{m} \times 40\ \mu\text{m}$), and the emission spectrum (F) of dendrimers **1** and **3** mixed (molar ratio, 5:5) nanofibers; NCAFM image (G, $50\ \mu\text{m} \times 50\ \mu\text{m}$), confocal fluorescence image (H, $40\ \mu\text{m} \times 40\ \mu\text{m}$), and the emission spectrum (I) of dendrimers **1** and **3** mixed (molar ratio, 9:1) nanofibers. All nanofibers are prepared by drop-casting a 2.0×10^{-6} M (total concentration) dendrimer solution in THF in a saturated environment of THF:H₂O = 90:10 (v/v) on a silicon surface.

mixing of dendrimer **1** and dendrimer **2**, the fluorescence emission spectrum shifts to the blue upon decreasing the relative concentration of **3**, indicating homogeneous mixing and the absence of phase separation.

Mechanistic Consideration of the Polyphenylene Dendrimer Nanofiber Formation. As discussed in a previous paper,^{36b} the driving force for the formation of polyphenylene dendrimer nanofibers is attributed to the π - π and van der Waals interactions among dendrimer branches. Polyphenylene dendrimers are characterized as shape-persistent molecules; this well-defined 3D structure may lead to interdigitation of parts of the polyphenylene dendrimers upon aggregation to maximize the intermolecular interactions. A dendrimer **1** tetramer model has been optimized (Figure 8), which suggests that interdigitation is favorable and could lead to a directional aggregation of dendrimer molecules. The dimer-like emission of dendrimer **2** when assembled in nanofibers points to the importance of shape-driven π - π

interactions stabilizing the nanofibers. The presence of two perylenemonoimide chromophores at the rim is already enough to cause steric crowding, limiting the directional growth which can be overcome by mixing with the nonsubstituted dendrimer **1**.

The formation of dendrimer nanofibers could either occur in the dendrimer solution during the solvent evaporation or proceed directly on the surface of substrate. Even though the mechanism of the nanofiber formation is not fully understood, the visualization of dendrimer nanofiber networks (some nanofibers being superimposed on the others) and their formation on various substrates such as HOPG, silicon, glass, and mica (which implies that the formation of dendrimer nanofibers are rather independent of the surface properties of the substrate) suggests that the former mechanism is more plausible. Light scattering has demonstrated that the polyphenylene dendrimer molecules aggregate into clusters in solution upon increasing concentration.⁴⁴

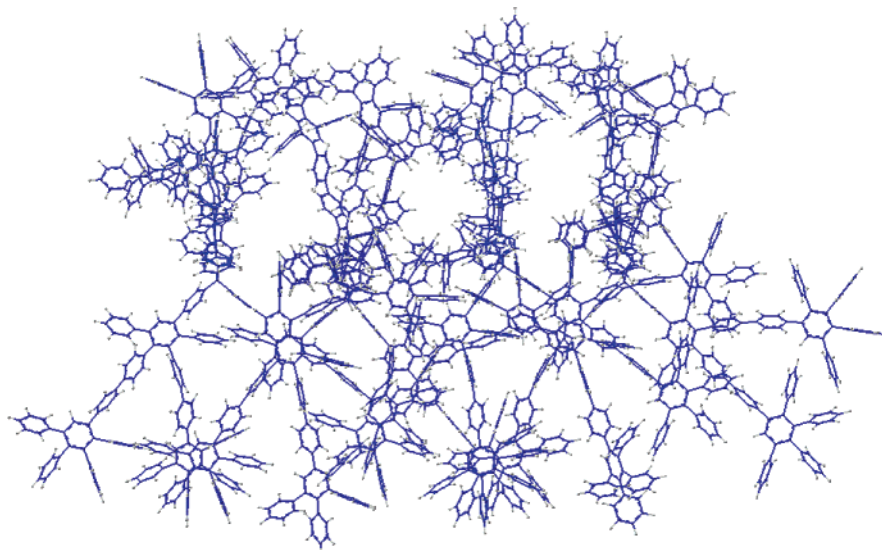


Figure 8. A tetramer model of dendrimer **1** built by the MMFF method.

Conclusion

Polyphenylene dendrimer **1** in different organic solvents exclusively self-assembles into nanofibers on various substrates upon drop-casting under a saturated solvent atmosphere. While nanofiber clusters are formed on a HOPG and silicon surface from its solution in CHCl_3 , dendrimer **1** self-assembles into a nanofiber network from a solution in THF on a silicon, glass, or mica surface, which distributes over the whole surface of the substrate. Addition of a small amount of water to the drop-casting THF atmosphere suppresses the nanofiber aggregation and gives rise to individual nanofibers. It has been demonstrated that the morphologies of the dendrimer **1** nanofibers can be regulated by changing solvent, substrate, and preparation method.

Fluorescent nanofibers can be prepared from a polyphenylene dendrimer with a fluorescent functional group either attached to its periphery or incorporated in its core. Polyphenylene dendrimer **2** with a perylenemonoimide chromophore attached to the periphery exclusively self-assembles into fluorescent nanofibers, which shows dimer-like emission. Polyphenylene dendrimer **4** with a perylenediimide core also self-assembles into fluorescent nanofibers, but the dendrimer arms shield the perylenediimide core. Mixtures of nonfluorescent dendrimer **1** and fluorescent dendrimers **2** or **3** lead to the exclusive formation of fluorescent nanofibers. The emission spectrum of these nanofibers changes upon decreasing the relative concentration ratio of the fluorescent chromophore, indicating that the fluorescent dendrimers are homogeneously distributed within the nanofibers. Moreover, the nonfluorescent dendrimer **1** can act as a guest to coassemble otherwise non-fiber-forming dendrimers into micrometer long nanofibers.

The dimensions of these (functional) polyphenylene dendrimer nanofibers can to a certain extent be controlled. Their formation not only is expected to add new insight into the self-assembly parameters of dendrimers but also indicates that one can build in functionalities in these fibers. One of the challenges that remain to be solved is the stabilization of these fibers. One way to achieve this might be by introducing functionalities which could covalently link the dendrimers in the nanofibers after self-assembly.

Acknowledgment. The authors thank the DWTC through IUAP-V-03, the FWO (Flemish Ministry of Education), the STWW through the IWT project "Molecular Nanotechnology", the German Ministry of Education and Research, and the German Science Foundation (SFB 625). The collaboration was made possible thanks to a Max-Planck Research Award. S.D.F. is a postdoctoral fellow of the "Fonds voor wetenschappelijk onderzoek-Vlaanderen" (FWO).

References and Notes

- (1) Tomalia, D. A.; Naylor, A. M.; Goddard, W. A., III. *Angew. Chem., Int. Ed. Engl.* **1990**, *29*, 138.
- (2) Newkome, G. R.; Moorefield, C. N.; Vögtle, F. *Dendritic Molecules: Concepts, Synthesis, Perspectives*; VCH: Weinheim, 1996.
- (3) Berresheim, A. J.; Müller, M.; Müllen, K. *Chem. Rev.* **1999**, *99*, 1747.
- (4) (a) Greyson, S. M.; Fréchet, J. M. J. *Chem. Rev.* **2001**, *101*, 3819. (b) Tomalia, D. A.; Fréchet, J. M. J. *J. Polym. Sci., Polym. Chem.* **2002**, *40*, 2719.
- (5) Tsukruk, V. V. *Adv. Mater.* **1998**, *10*, 253.
- (6) Smith, D. K.; Diederich, F. *Top. Curr. Chem.* **2000**, *210*, 183.
- (7) Emrick, T.; Fréchet, J. M. J. *Curr. Opin. Colloid Interface Sci.* **1999**, *4*, 15.
- (8) Tully, D. C.; Fréchet, J. M. J. *Chem. Commun.* **2001**, 1229.
- (9) Zeng, F.; Zimmerman, S. C. *Chem. Rev.* **1997**, *97*, 1681.
- (10) Tomalia, D. A.; Majoros, I. In *Supramolecular Polymers*; Liferri, A., Ed.; Marcel Dekker: New York, 2000; p 359.
- (11) Köhn, F.; Hofkens, J.; Wiesler, U.-M.; Cotlet, M.; van der Auweraer, M.; Müllen, K.; De Schryver, F. C. *Chem.-Eur. J.* **2001**, *7*, 4126.
- (12) Watanabe, S.; Regen, S. L. *J. Am. Chem. Soc.* **1994**, *116*, 8855.
- (13) (a) Tsukruk, V. V.; Rinderspacher, F.; Bliznyuk, V. N. *Langmuir* **1997**, *13*, 2171. (b) Bliznyuk, V. N.; Rinderspacher, F.; Tsukruk, V. V. *Polymer* **1998**, *39*, 5249.
- (14) Yoon, H. C.; Kim, H. S. *Anal. Chem.* **2000**, *72*, 922.
- (15) Khopade, A.; Caruso, F. *Nano Lett.* **2002**, *2*, 415.
- (16) Wang, J.; Jia, X.; Zhong, H.; Luo, Y.; Zhao, X.; Cao, W.; Li, M. *Chem. Mater.* **2002**, *14*, 2854.
- (17) (a) Zhao, M.; Tokuhisa, H.; Crooks, R. M. *Angew. Chem., Int. Ed. Engl.* **1997**, *36*, 2596. (b) Tokuhisa, H.; Zhao, M.; Baker, L. A.; Phan, V. T.; Dermody, D. L.; Garcia, M. E.; Peez, R. F.; Crooks, R. M.; Mayer, T. M. *J. Am. Chem. Soc.* **1998**, *120*, 4492. (c) Hierlemann, A.; Campbell, J. K.; Baker, L. A.; Crooks, R. M.; Ricco, A. J. *J. Am. Chem. Soc.* **1998**, *120*, 5323. (d) Lackowshi, W. M.; Campbell, J. K.; Edwards, G.; Chechik, V.; Crooks, R. M. *Langmuir* **1999**, *15*, 7632.
- (18) Rahman, K. M. A.; Durning, C. J.; Turro, N. J.; Tomalia, D. A. *Langmuir* **2000**, *16*, 10154.

- (19) Zhang, H.; Grim, P. C. M.; Liu, D.; Vosch, T.; De Feyter, S.; Wiesler, U.-M.; Berresheim, A. J.; Müllen, K.; Van Haesendonck, C.; Vandamme, N.; De Schryver, F. C. *Langmuir* **2002**, *18*, 1801.
- (20) (a) Schlupp, M.; Weil, T.; Berresheim, A. J.; Wiesler, U. M.; Bargon, J.; Müllen, K. *Angew. Chem., Int. Ed.* **2001**, *40*, 4011. (b) Vossmeier, T.; Guse, B.; Besnard, I.; Bauer, R. E.; Müllen, K.; Yasuda, A. *Adv. Mater.* **2002**, *14*, 238.
- (21) Emmrich, E.; Franzka, S.; Schmid, G. *Nano Lett.* **2002**, *2*, 1239.
- (22) (a) Tully, D. C.; Wilder, K.; Fréchet, J. M. J.; Trimble, A. R.; Quate, C. F. *Adv. Mater.* **1999**, *11*, 314. (b) Tully, D. C.; Trimble, A. R.; Fréchet, J. M. J. *Chem. Mater.* **1999**, *11*, 2892.
- (23) Li, H.; Kang, D.-J.; Blamire, M. G.; Huck, W. T. S. *Nano Lett.* **2002**, *2*, 347.
- (24) McKendry, R.; Huck, W. T. S.; Weeks, B.; Fiorini, M.; Abell, C.; Rayment, T. *Nano Lett.* **2002**, *2*, 713.
- (25) Wu, X. C.; Bittner, A. M.; Kern, K. *Langmuir* **2002**, *18*, 4984.
- (26) (a) Uppuluri, S.; Swanson, D. R.; Piehler, L. T.; Li, J.; Hagnauer, G. L.; Tomalia, D. A. *Adv. Mater.* **2000**, *12*, 796. (b) Betley, T. A.; Hessler, J. A.; Mecke, A.; Manaszak Holl, M. M.; Orr, B. G.; Uppuluri, S.; Tomalia, D. A.; Baker, J. R., Jr. *Langmuir* **2002**, *18*, 3127.
- (27) (a) Hudson, S. D.; Jung, H. T.; Percec, V.; Cho, W. D.; Johansson, G.; Ungar, G.; Balagurusamy, V. S. K. *Science* **1997**, *278*, 449. (b) Percec, V.; Ahn, C. H.; Ungar, G.; Yeardley, D. J. P.; Möller, M.; Sheiko, S. S. *Nature (London)* **1998**, *391*, 161. (c) Percec, V.; Ahn, C. H.; Cho, W. D.; Jamieson, A. M.; Kim, J.; Leman, T.; Schmidt, M.; Gerle, M.; Möller, M.; Prokhorova, S. A.; Sheiko, S. S.; Cheng, S. Z. D.; Zhang, A.; Ungar, G.; Yeardley, D. J. P. *J. Am. Chem. Soc.* **1998**, *120*, 8619. (d) Percec, V.; Cho, W. D.; Ungar, G.; Yeardley, D. J. P. *Angew. Chem., Int. Ed.* **2000**, *39*, 1597. (e) Percec, V.; Cho, W. D.; Möller, M.; Prokhorova, S. A.; Ungar, G.; Yeardley, D. J. P. *J. Am. Chem. Soc.* **2000**, *122*, 4249. (f) Yeardley, D. J. P.; Ungar, G.; Percec, V.; Holerca, M. N.; Johansson, G. *J. Am. Chem. Soc.* **2000**, *122*, 1684. (g) Percec, V.; Cho, W. D.; Ungar, G. *J. Am. Chem. Soc.* **2000**, *122*, 10273. (h) Percec, V.; Cho, W. D.; Ungar, G.; Yeardley, D. J. P. *J. Am. Chem. Soc.* **2001**, *123*, 1302. (i) Percec, V.; Holerca, M. N.; Uchida, S.; Cho, W. D.; Ungar, G.; Lee, Y.; Yeardley, D. J. P. *Chem.—Eur. J.* **2002**, *8*, 1106. (j) Percec, V.; Glodde, M.; Bera, T. K.; Miura, Y.; Shiyanovskaya, I.; Singer, K. D.; Balagurusamy, V. S. K.; Heiney, P. A.; Schnell, I.; Rapp, A.; Spiess, H. W.; Hudson, S. D.; Duan, H. *Nature (London)* **2002**, *19*, 6905.
- (28) Masuo, S.; Yoshikawa, H.; Asahi, T.; Masuhara, H. *J. Phys. Chem. B* **2001**, *105*, 2885.
- (29) Schlüter, A. D.; Rabe, J. P. *Angew. Chem., Int. Ed.* **2000**, *39*, 864.
- (30) Müllen, K.; Wegner, G. *Electronic Materials: The Oligomer Approach*; Wiley-VCH: Weinheim, 1998.
- (31) (a) Herwig, P.; Kayser, C. W.; Müllen, K.; Spiess, H. W. *Adv. Mater.* **1996**, *8*, 510. (b) Schmidt-Mende, L.; Fechtenkötter, A.; Müllen, K.; Moons, E.; Friend, R. H.; MacKenzie, J. D. *Science* **2001**, *293*, 1119.
- (32) Wiesler, U. M.; Berresheim, A. J.; Morgenroth, F.; Lieser, G.; Müllen, K. *Macromolecules* **2001**, *34*, 187.
- (33) Zhang, H.; Grim, P. C. M.; Foubert, P.; Vosch, T.; Vanoppen, P.; Wiesler, U. M.; Berresheim, A. J.; Müllen, K.; De Schryver, F. C. *Langmuir* **2000**, *16*, 9009.
- (34) Wind, M.; Wiesler, U. M.; Saalwächter, K.; Müllen, K.; Spiess, H. W. *Adv. Mater.* **2001**, *13*, 752–756.
- (35) (a) Loi, S.; Wiesler, U. M.; Butt, H. J.; Müllen, K. *Chem. Commun.* **2000**, 1169. (b) Loi, S.; Wiesler, U. M.; Butt, H. J.; Müllen, K. *Macromolecules* **2001**, *34*, 3661. (c) Loi, S.; Butt, H. J.; Hampel, C.; Bauer, R.; Wiesler, U. M.; Müllen, K. *Langmuir* **2002**, *18*, 2398.
- (36) (a) Liu, D.; Zhang, H.; Grim, P. C. M.; De Feyter, S.; Wiesler, U. M.; Berresheim, A. J.; Müllen, K.; De Schryver, F. C. *Langmuir* **2002**, *18*, 2385. (b) Liu, D.; De Feyter, S.; Grim, P. C. M.; Vosch, T.; Grebel-Köhler, D.; Wiesler, U. M.; Berresheim, A. J.; Müllen, K.; De Schryver, F. C. *Langmuir* **2002**, *18*, 8283.
- (37) (a) Weil, T.; Wiesler, U.-M.; Herrmann, A.; Bauer, R.; Hofkens, J.; De Schryver, F. C.; Müllen, K. *J. Am. Chem. Soc.* **2001**, *123*, 8101. (b) Lor, M.; De, R.; Jordens, S.; De Belder, G.; Schweitzer, G.; Cotlet, M.; Hofkens, J.; Weil, T.; Herrmann, A.; Müllen, K.; Van Der Auweraer, M.; De Schryver, F. C. *J. Phys. Chem. A* **2002**, *106*, 2083–2090.
- (38) Herrmann, A.; Weil, T.; Sinigersky, V.; Wiesler, U.-M.; Vosch, T.; Hofkens, J.; De Schryver, F. C.; Müllen, K. *Chem.—Eur. J.* **2001**, *7*, 4844.
- (39) Cotlet, M.; Hofkens, J.; Habuchi, S.; Dirix, G.; Van Guyse, M.; Michiels, J.; Vanderleyden, J.; De Schryver, F. C. *Proc. Natl. Acad. Sci. U.S.A.* **2001**, *98*, 14398.
- (40) Halgren, T. A. *J. Comput. Chem.* **1996**, *17*, 490.
- (41) Fondecave, R.; Wyart, F. B. *Macromolecules* **1998**, *31*, 9305.
- (42) Maus, M.; Mitra, S.; Lor, M.; Hofkens, J.; Weil, T.; Herrmann, A.; Müllen, K.; De Schryver, F. C. *J. Phys. Chem. A* **2001**, *105*, 3961.
- (43) Liu, D.; De Feyter, S.; Cotlet, M.; Stefan, A.; Wiesler, U.-M.; Herrmann, A.; Grebel-Koehler, D.; Qu, J.; Müllen, K.; De Schryver, F. C. *Macromolecules*, in press.
- (44) Fytas, G. Private communication.

MA0348573